Biotechnology and Bioprocess Engineering 21: 305-313 (2016)
DOI 10.1007/s12257-015-0628-5

RESEARCH PAPER

Bioanode of Polyurethane/Graphite/Polypyrrole Composite in Microbial Fuel Cells

Pedro Pérez-Rodríguez, Víctor M. Ovando-Medina, Silvia Y. Martínez-Amador, and José A. Rodríguez-de la Garza

Received: 30 September 2015 / Revised: 25 January 2016 / Accepted: 22 February 2016

Abstract Polyurethane (PU) foams were coated with graphite, and pyrrole monomer was subsequently polymerized onto its surface by chemical oxidization to obtain nanostructured polyurethane/graphite/polypyrrole (PU/Graph/PPy) composites, which were used for anaerobic microorganisms grown and tested as anodes in microbial fuel cells (MFC) using municipal wastewater as fuel. The effects of oxidizing agent type (ammonium persulfate and $FeCl_3$) used in pyrrole polymerization on the performance of electrodes in MFC were studied. Composites were characterized by Fourier Transform Infrared (FTIR) spectroscopy, Scanning Electron Microscopy (SEM), and by the four-point probes to determine conductivity. It was observed from SEM analysis that globular nanostructures of PPy were formed onto PU surface with average diameters between 120 and 450 nm, which are typical of aqueous polymerization of pyrrole monomer. The highest output power density observed in MFCs was 305.5 mW/m^3 for the composite synthesized using $FeCl_3$ as the oxidant, and 128.6 mW/m^3 using the composite obtained with ammonium persulfate as oxidizing; the corresponding chemical oxygen demand (COD) removal were 48.2 and 45.5%, respectively. The calculated coulombic efficiency for PU/Graph/PPy composite obtained with $FeCl_3$ as oxidant was of 9.4%. Internal resistance of MFC using the composite obtained with $FeCl_3$ as oxidant was determined by linear sweep voltammetry (LSV) and the variable resistance (VR) methods, giving 4.8 and 2.9 kΩ, respectively, with average maximum power density of 237.5 mW/m^3.

Keywords: polyurethane, polypyrrole, graphite, microorganism, MFC

Pedro Pérez-Rodríguez, Silvia Y. Martínez-Amador
Departamento de Botánica, Universidad Autónoma Agraria Antonio Narro. Calzada Antonio Narro 1923, Buenavista, Saltillo, Coahuila 25315, México

Víctor M. Ovando-Medina*
Ingeniería Química, COARA – Universidad Autónoma de San Luis Potosí, Carretera a Cedral KM 5+600, San José de las Trojes, Matehuala, SLP, México 78700
Tel: +52-48-8125-0150; Fax: +52-48-8125-0150
E-mail: ovandomedina@yahoo.com.mx

José A. Rodríguez-de la Garza
Departamento de Biotecnología, Facultad de Ciencias Químicas, Universidad Autónoma de Coahuila. José Cárdenas Valdez y Venustiano Carranza S/N, Col. República Oriente, Saltillo, Coahuila 25280, México

1. Introduction

MFCs are energy producer systems in which chemical energy is directly transformed into electrical energy by the catalytic activity of electroactive microorganisms [1]. MFC have become one of the most promising techniques for alleviating energy deficiency and environmental pollution at the same time because of their clean, sustainable, and renewable nature [2-4]. MFC use metabolism of exoelectrogens, microorganisms that mediate extracellular electron transfer, to convert chemical energy into electrical energy [5]. Therefore, in MFC, the performance is controlled by electroactive bacteria attached to the anode surface to form biofilms rather than planktonic microorganisms [6]. Therefore, as Yuan *et al.* [7] stated, the anode as the material electron transfer and as the support for biofilm formation is a key component in determining power generation. Generally, the anode will perform better if the anode material has a greater specific surface area and higher affinity for bacterial cells (good microorganism compatibility).

Since a practical point of view, anodes in MFC have to accomplish at least four requisites: low-cost, easy preparation/synthesis, affinity of microorganism by the anode surface,

and high current collection. In this sense, a wide variety of materials and configurations have been studied for the anode, such as carbonaceous, metal and metal oxides, and composite materials [8,9]. For that reasons, researches are directed towards the preparation and characterization of new electrodes with advanced materials. For example, Yuan and Kim [10] prepared conductive carbon paper sheet by immersing carbon paper into a polypyrrole/carbon black composite dispersion, and also by electropolymerization of pyrrole onto the carbon paper sheet. They immobilized *Proteus vulgaris* (aerobically grown and suspended in a phosphate buffer solution pH of 7.0) onto this material and used as anode in a small MFC with glucose as fuel. These authors observed that MFC performance increased when the anode was coated with carbon black or polypyrrole, achieving the best performance (452 mW/m^2 of power density) when polypyrrole/carbon black composite material was coated onto a carbon paper electrode. Yuan *et al*. [7] used a vegetable sponge, obtained from the fruit of a plant named *loofah*, as anode in MFC. Sponges were previously carbonized or, coated with polyaniline (PANI) and carbonized to obtain nitrogen enriched carbon nanoparticles deposited onto sponges. They used preacclimated bacteria (sample taken from a running MFC) from activated anaerobic sludge and, sodium acetate as carbon source and a culture medium (NaH_2PO_4, NH_4Cl, KCl, vitamin stock solution, and a mineral stock solution); obtaining a power density of approximately 1,000 mW/m^2 using the PANI coated loofah sponge. Patil *et al.* [11] deposited PANI onto a graphite electrode and used as anode in a MFC to immobilize electrochemically active microbes (*Enterobacter aerogenes*) using activated sludge as inoculum and dairy waste (collected from a local dairy industry) as fuel. A voltage of 1.02 V was observed with modified graphite electrode, compared with unmodified graphite, which produced 0.48 V.

The synthesis of composites of PU with semiconducting polymers has been previously reported. For example, Choi *et al.* [12] reported the synthesis of PU and deposition of PPy by chemical oxidation of pyrrole onto its surface to be used as actuators. Broda *et al.* [13] obtained conducting composite of PPy nanoparticles and PU for tissue engineering; from the cytocompatibility assay data, they observed minimal cytotoxic effect of composites. Chiu *et al*. [14] polymerized pyrrole electrochemically in a matrix of PU. By this procedure, it was observed that PPy grew in a treelike structure, with molecular chains spreading from the electrode surface into the solution. Also, the transition temperature of PU/PPy composite increased with PPy content. PU has been also coated and mixed with others semiconducting polymers like polyaniline (PANI) as reported by Bouanga *et al.* [15] who studied the electrical properties of PU/PANI composite obtained by chemical oxidation of aniline inside of a previously swelled PU film. They observed a relaxation process of composite explained in terms of interfacial polarization due to the double-layered structure of composite film. Rangel-Vazquez *et al*. [16] synthesized and characterized copolymer of PU and PANI. These authors proposed a morphological interpretation in which PANI chains formed a phase dispersed in a PU matrix, linked together by an interphase that could be responsible for the connectivity between the two polymers and determine excellent mechanical properties. However, only few works have been reported using composites of PU/semiconducting materials with immobilized micro-organism as anodes in MFC. Xie *et al.* [5,17] used anodes of carbon nanotubes and graphene deposited onto PU foams and stainless steel sheets as current collector in MFC, achieving 1.24 and 1.57 W/m^2 for carbon PU/nanotubes and PU/graphene composites, respectively. In a previous work, our research group [18] demonstrated that coating a PU foam matrix with semiconducting copolymer of PPy and PANI, the microorganism grown can be increased due to better compatibility of microorganisms with the surface of PU/(PPy-co-PANI) composite and increased superficial area, and used as filler in continuous flow packed-bed reactors for wastewater treatment with chemical oxygen demand removal efficiencies up to 94%.

As can be seen, semiconducting polymers as PPy can be used to increase microorganism biocompatibility with a surface as PU, and work as current collector in MFCs. Therefore, in this work, composites of PU/Graph/PPy were obtained by chemical oxidation of pyrrole monomer. Composites were used for microorganism grown onto its surface and tested in municipal wastewater treatment into a MFC. To the best of our knowledge, this is the first time that composites of PU/Graph/PPy are used to grow microorganism and used as anode in MFC with a municipal wastewater as carbon source.

2. Materials and Methods

2.1. Materials

Pyrrole (> 98%), $FeCl_3 \cdot 6H_2O$ (> 97%) and ammonium persulfate (APS, > 98%) were purchased from Sigma-Aldrich (Toluca, Mexico) and used as received. Polyurethane foam (PU) was purchased from a local market in Saltillo, Mexico. Graphite (aerosol) was acquired from CRC Industrial™ (Dry Graphite Lube) and used as received. Distilled water was used in all polymerizations. Reagents used for chemical oxygen demand (COD) determinations were: sulfuric acid (96 ~ 98%), potassium dichromate (96 ~ 98%) purchased from ANALYTYKA (Saltillo, Mexico); mercuric sulfate (> 98%) and silver sulfate (> 98%), from

Table 1. Amounts in grams of reactants used in electrodes preparation

Electrode	Pyrrole	Graphite*	$FeCl_3 \cdot 6H_2O$	APS
PU/Graph/PPy-APS	0.25	0.025		0.8443
PU/Graph/PPy-$FeCl_3$	0.25	0.025	2.002	

*Average amounts attached to PU foam after graphite coating, washing and drying.

JALMEK CIENTIFICA, S.A. DE C.V., and potassium biphtalate (> 99.95%) from FERMONT (Monterrey, Mexico). Ion exchange membrane used for MFC was acquired from Aldrich (Nafion® 117, thickness 0.007 in.).

2.2. Preparation of PU/Graph/PPy anodes

PU foam was cut in pieces of 3 cm × 3 cm × 0.8 cm and washed with distilled water and acetone to remove impurities and then dried at 80°C for 2 h. After that, three homogeneous layers of aerosol graphite were applied onto PU foams. PU/Graph foams were dried at room temperature through 2 h and washed with distilled water to remove non-attached graphite and, dried again at 80°C for 2 h. Table 1 shows the compositions used in the preparation of each electrode. Polymerizations of pyrrole onto PU/Graph foams were made as follows: 100 mL of distilled water were mixed with 0.25 g (3.7 mmol) of pyrrole monomer under magnetic stirring in a baker of 250 mL. Afterwards, the PU/Graph foams were immersed in the solution and the air bubble were extracted and allowed to saturate with pyrrole through 1 h under magnetic stirring. Then, to start polymerizations, the oxidizing agent (APS or $FeCl_3$) dissolved in 5 mL of distilled water was added to the reaction mixture, allowing to proceed polymerizations by 2 h. The resulting PU/Graph/PPy electrodes were washed gently with distilled water and dried at 60°C through 24 h. Amounts of polypyrrole attached to PU/Graph foam were determined by gravimetry from a mass balance as $CP = (W_f - W_i)/W_f \times 100$, where CP represents the % of PPy in the material of PU/Graph/PPy, W_f is the final dried weight of foam after polymerization of pyrrole, and W_i is the initial dried weight of PU/Graph foams.

2.3. Microorganism grown onto composites

Biofilm formation onto electrodes was made as follows: each electrode was immersed in 200 mL of municipal wastewater (from a wastewater treatment plant) and mixed with 100 mL of degranulated anaerobic sludge (from a UASB reactor in the wastewater treatment plant of a brewery in Monterrey, Mexico). Reactors were in batch regime for 15 days at 35°C under anaerobic conditions for biofilm formation. Each two days, reactors were gently stirred to homogenize it. Afterwards, the supernatant was removed along with the excess of sludge to use the electrodes with biofilm in MFC. Uncoated PU foam was prepared in a similar way for comparison.

2.4. Chemical and morphological characterization

PU foam and electrodes of PU/Graph/PPy-APS and PU/Graph/PPy-$FeCl_3$ were analyzed by FTIR spectroscopy (Agilent Tech., Cary 630) to determine chemical compositions, and by scanning electron microscopy (SEM) (FEI, Quanta-3D FEG) to know surface morphology of composites before and after microorganism colonization. Determinations of COD removal during anaerobic wastewater treatment were made as follows: the aqueous samples were centrifuged (SOLBAT J-600 Centrifuge) at 3,000 rpm for 3 min before testing, using the supernatant to evaluate COD. COD was measured as soluble by the closed reflux colorimetric method in accordance with Standard Methods [19] and NMX-AA-030-SCFI-2001 [20]: 2.5 mL of samples, standards (potassium biphtalate dilutions) and blanks (distilled water) were heated to 150 ± 2ºC in a closed reactor (HACH, Digital Reactor Block 200) for 2 h in the presence of acid dichromate solution (3.5 mL of a solution of silver sulfate dissolved in sulfuric acid, and 1.5 mL of a solution of potassium dichromate, mercuric sulfate and sulfuric acid, dissolved in distilled water). The tubes were then cooled down and measured at 600 nm on a HACH Spectrophotometer (DR 5000).

2.5. MFC arrangement

Fig. 1 shows a diagram of the arrangement of MFC used in the experiments. It consisted of PU/Graph/PPy anode with microorganisms colonization (biofilm) filled with 50 mL of fresh domestic wastewater as fuel and in anaerobic conditions. The cathodic compartment was filled with 50 mL of a solution 50 mM of $K_3[Fe(CN)_6]$, and a cathode of a stainless steel sheet (3 cm × 3 cm × 0.2 cm). A stainless steel rod was attached to each electrode for electron collection and connected to an external resistance of 1.0 kW. Both compartment were separated by a proton exchange membrane (4 cm × 4 cm) previously hydrated (sequentially boiled for 1 h in H_2O_2 (30%), deionized water, 0.5 M H_2SO_4, and deionized water). MFC were placed into an incubator at 35°C. A sample of wastewater was collected at the end of experiments from the anodic compartment to determine COD removal. Voltage generation (V) was measured with a digital multimeter (Fluke 289, Trendcapture). The polarization and power density curves

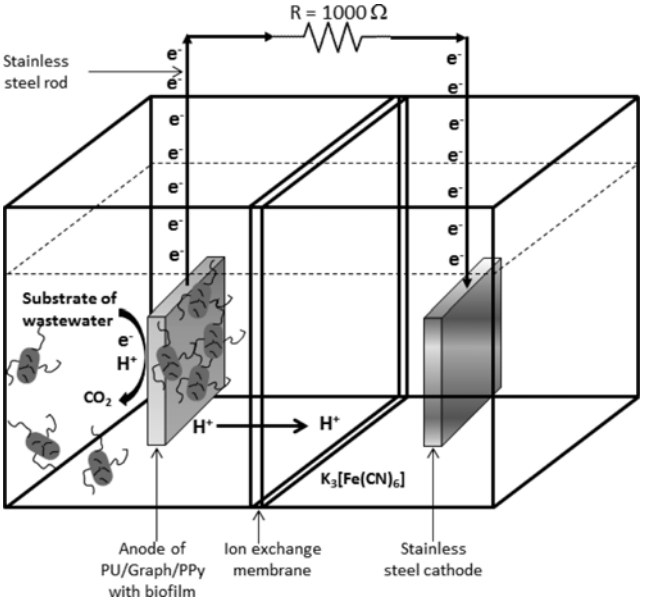

Fig. 1. Diagram of the arrangement of MFC used in the experiments.

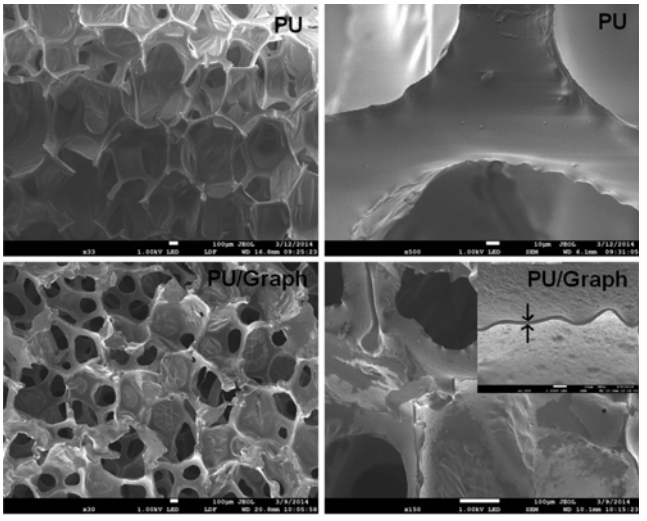

Fig. 2. SEM images of PU foam and PU/Graph at different magnifications.

by the VR method were measured by varying the load resistance from 50×10^{-3} to 100 kΩ when the MFC reached a stable output voltage. LSV was done using a potentiostat/galvanostat (Gamry G300) at the recommended scan rate of 1 mV/sec starting from the measured open circuit potential [21,22]. Power density by LSV and VR methods were normalized with the anodic compartment volume in m^3. Electrodes configuration was as follows: the anode of MFC was used as the counter and reference electrode, and the cathode as working [23]. The current and power outputs were normalized to the volume of anodic compartment of MFC.

To establish the amount of biomass attached to the supports, assessments were carried out as follows: The colonized supports were removed from MFC, dried at 105ºC for 24 h and weighted. This value was compared with the weight of the support before used in MFC, obtaining the biomass weight in mg per gram of clean support.

3. Results and Discussion

There are many factors that can affect the MFCs performance (electrode materials, solution ionic strength, chemical substrate, electrode spacing, internal and external cell resistance, *etc.*) but it is well recognized that the anode with the attached microorganisms has the highest impact on power density and wastewater treatment efficiency [24]. In the past few years, some researchers have studied the anode material and its structure by increasing its specific surface area and conductivity, because these factors can directly affect the bacteria attachment, electron transfer and substrate oxidation [25]. Table 2 shows the amounts of graphite and polypyrrole attached to the PU foam, and conductivity after the synthesis. It can be seen that there is practically no difference on the quantity attached of this compounds between the studied treatments, however, conductivity value of PU/Graph/PPy-$FeCl_3$ electrode was almost five magnitude orders higher than that observed for PU/Graph/PPy-APS. Even though both treatments had the same components, the presence of ferric chloride ($FeCl_3$) in small amounts remaining after washing can considerably act as a doping agent increasing the conductivity of this composite.

Fig. 2 shows the SEM images at different magnifications of PU foams before and after coating with graphite layers. It can be seen that PU foam consisted of homogeneous surface of well-defined pores with average diameter of 600 μm. Sample of PU/Graph shows some slightly occluded pores, with an average thickness of graphite layer of approximately 2 μm (arrows in the inset of Fig. 2). As can be seen in Fig. 3, after pyrrole polymerization using APS as oxidant, the initial PU foam pores became highly

Table 2. Amounts of graphite and polypyrrole attached to PU foam

Electrode	Graphite (%)	PPy (%)	Conductivity (S/m)
PU/Graph/PPy-APS	44.9	23.1	9.4×10^{-7}
PU/Graph/PPy-$FeCl_3$	46.1	24.3	2.4×10^{-2}

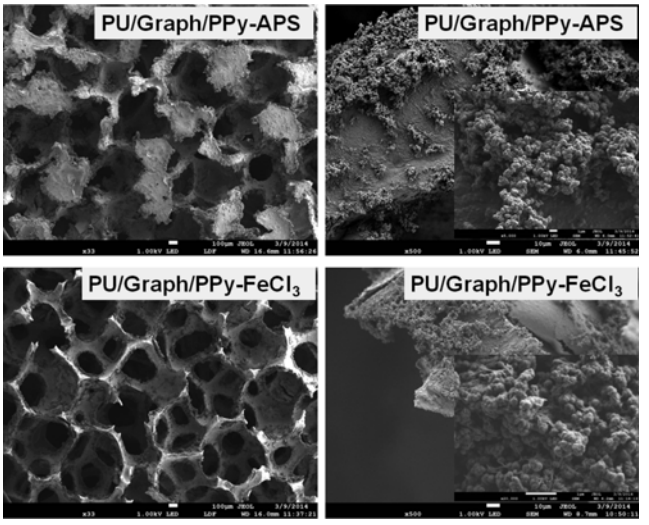

Fig. 3. SEM images of PU/Graph/PPy composites prepared using APS and $FeCl_3$ as oxidizing agents at different magnifications.

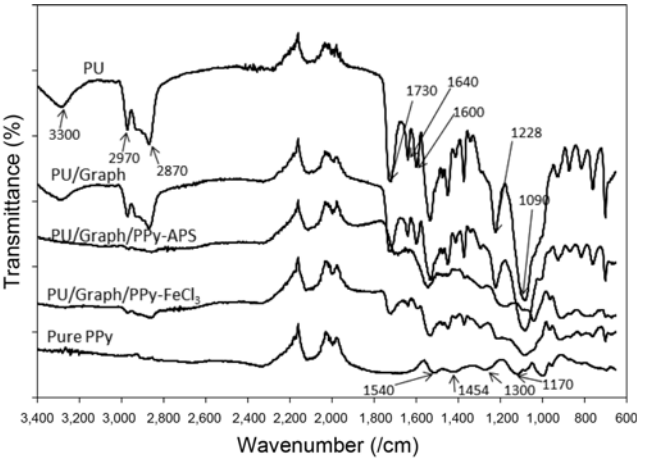

Fig. 4. FTIR spectra of composites of PU/Graph/PPy and its comparison with uncoated PU foam, PU/Graph, and pure PPy.

occluded and globular structures of PPy were formed with diameters ranging from 280 to 450 nm, which is typical of PPy formation in aqueous dispersion without the presence of any surfactants. When $FeCl_3$ was used as the oxidant, less occluded PU foam pores can be observed, and not only globular nanostructures with smaller diameters than that observed using APS as oxidant, ranging between 120 and 250 nm, but also fiber-like structures (Inset in Fig. 3 and arrows in Fig. S8 of electronic supplementary information) of 200 ~ 800 nm in large, connecting the globular nanostructures. Due to PPy morphology coating PU foam, increased surface area can be obtained, so that more microorganisms and organic molecules can have access to the modified surface. More importantly, positively charged nature of PPy, increases adhesion of negatively charged bacteria to the surface through electrostatic attraction [18,26,27].

The attachment of biomolecules or biologically active species to conductive nanostructures is a critical step in order to achieve its biofunctionality. The development of flexible designs that combines the structural features of nanostructured conductive polymers with the biofunctionality and biocompatibility required for the application is still considered the principal task in creating feasible bioactive systems [18,28]. Combining mechanical properties of PU with biocompatibility of PPy, results in a material that can be used for microorganism colonization for applications like wastewater treatment and energy production using MFCs.

Fig. 4 shows the FTIR spectra of different materials synthesized and that of uncoated PU foam. The spectrum of PU foam shows the typical signal of toluene diisocyanate groups (TDI); signals at 1730 and at 1640/cm are ascribed to C=O stretching in urethane units, signal at 1600/cm is attributable to C=C of aromatic ring, signal at 1228/cm is ascribed to C-O, peak at 1090/cm can be attributed to C-O-C [29], which demonstrates that a TDI was used in the PU foam production. It can be also observed that intensities of signals of PU foam at 3300 and at 2970/cm decrease with graphite presence and disappear after coating with PPy. On the other hand, signals of PPy in composites of PU/Graph/PPy are observed at 1454/cm (C-C, ring stretching), 1540 (C=C, backbone stretching), 1300/cm (C-H in-plane) and, at 1170 /cm (C-N, stretching vibrations). The differences in conductivity between synthesized electrodes (using APS and $FeCl_3$ as oxidants) can be explained by comparison of signals of PPy at 1540 and at 1454/cm as follows: A higher ratio of these two peaks (C=C/C-C) represents higher conductivity because of longer effective π-conjugation along the PPy chains [30]. The integrated ratio intensities of C=C/C–C for PU/Graph/PPy-APS was 1.29, whereas the corresponding value for PU/Graph/PPy-$FeCl_3$ was 1.32, which confirms the higher conductivity value. These results imply that the use of $FeCl_3$ as oxidant, not only increases conductivity due to a doping effect, but also due to morphology (smaller particle diameters and fiber-like nanostructures, as shown in Fig. S8 of electronic supplementary information) and chemical structure of PPy chains.

Previously to test the synthesized electrodes in the MFCs, the COD removal in batch reactors were determined. Fig. 5 shows the profile of COD removal as a function of time of the wastewater treated using the different composites after microorganism colonization. It can be seen that after 2 days of degradation, COD decreases relatively fast from 480 to 368 mg/L when using pure PU foam and, from 440 to 335 mg/L for PU/Graph/PPy-APS and to 357 mg/L for PU/Graph/PPy-$FeCl_3$ composites. After ten days of treatment, COD removal behavior for PU foam and PU/

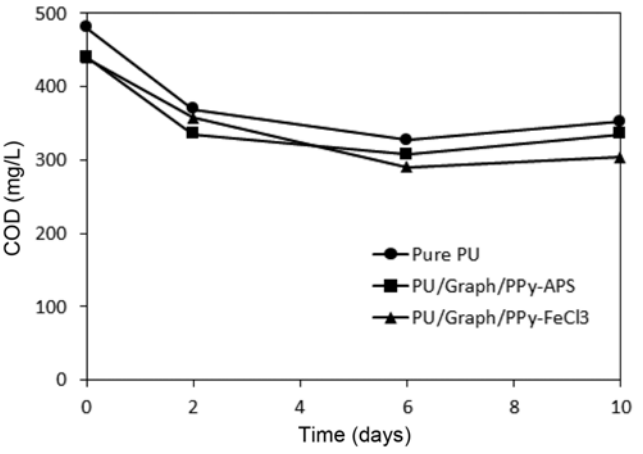

Fig. 5. COD removal profile using the synthesized PU foam composites.

Graph/PPy-APS was very similar, but slightly higher COD removal can be achieved by using PU/Graph/PPy-$FeCl_3$ material. This implies that PPy nanostructure obtained with $FeCl_3$ and electrical properties enhance microorganism colonization to this material. In the case of PU/Graph/PPy-APS, occluded pores were observed, giving negative results in COD removal, even similar to pure PU. Optimized morphology of surface was achieved for PU/Graph/PPy-$FeCl_3$, in which pores of PU structures were not so occluded and globular morphology with enhanced superficial area was observed, and more microorganisms can be immobilized. In this sense, cell densities of supports determined as mg of biomass per gram of clean support were 0.119 mg/g for PU, 0.074 mg/g for PU/Graph/PPy-APS, and 0.077 mg/g for PU/Graph/PPy-$FeCl_3$; namely, composites showed 38 and 35% less than pure PU, however PU/Graph/PPy-$FeCl_3$ showed just 3% higher of attached biomass than PU/Graph/PPy-APS.

The performance of PU foam, PU/Graph/PPy-APS and PU/Graph/PPy-$FeCl_3$ as MFC anodes were evaluated. Fig. 6 shows the power density (P) generated by the MFCs as a function of time in mW/m^3 calculated as $P = V^2/R_{ext}$, where R_{ext} is the external resistance, and V is the observed potential at different times. Fig. 6 (inset) also shows the percentage of COD removal at the end of MFC operation. It can be observed in all cases that maximum output power density is reached after 36 h of MFCs operation, and decreased continuously until a constant power density value. The output power density observed at 36 h with PU/Graph/PPy-$FeCl_3$ and PU/Graph/PPy-APS anodes were 23.2 times higher (~305.5 mW/m^3) and 9.8 times (~128.6 mW/m^3) higher than that observed for pure PU foam (13.1 mW/m^3), respectively. However, the output power density of PU/Graph/PPy-$FeCl_3$ was 2.4 times higher than the value for PU/Graph/PPy-APS. Similarly, COD removal percentage for PU/Graph/PPy-$FeCl_3$ and PU/Graph/PPy-APS were 38.5 and 30.7% higher than with uncoated PU foam (Inset in Fig. 6).

To determine the fraction of the electrons from converted organic matter that end up in the electrical circuit, the coulombic efficiency (ε_{Cb}) was evaluated. Data of voltage in Fig. 6 were converted to current (not shown here) using the relationship of $I = V/R_{ext}$, where I represents the current in A, V and R_{ext} are the potential in Volts and the external resistance (1 kΩ), respectively. These data were used in the following equation to calculate coulombic efficiencies of MFCs [31]:

$$\varepsilon_{Cb} = \frac{M\int_0^t Idt}{Fb\,v_{An}\Delta COD} \quad (1)$$

where M is the molecular weight of oxygen, I is the current, F is Faraday's constant, b = 4 is the number of electrons

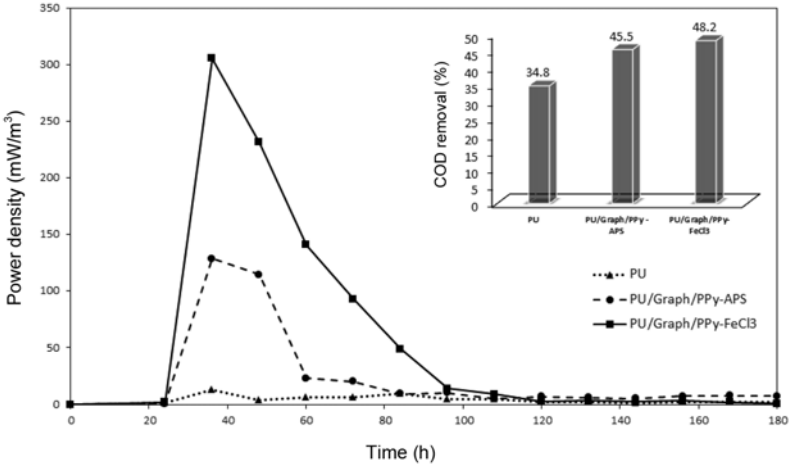

Fig. 6. Power density generated by the MFC as a function of time, and % of COD removal (inset) at the end of MFC operation.

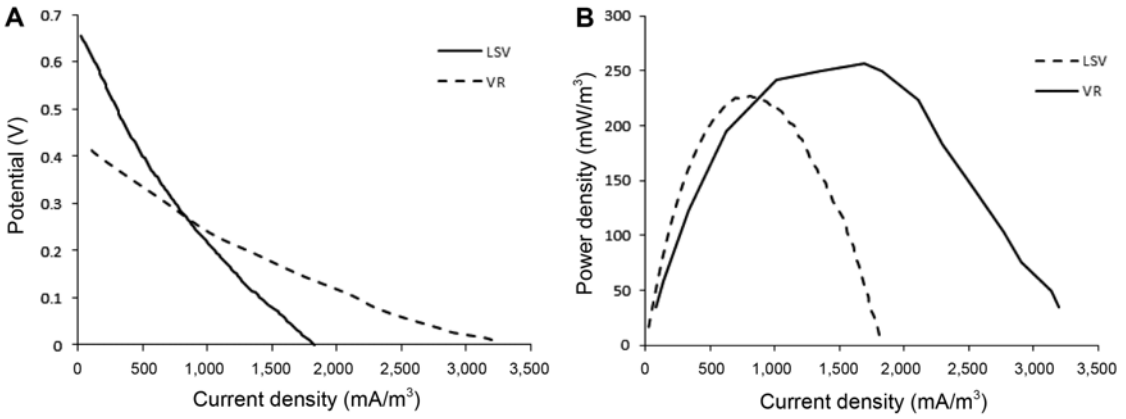

Fig. 7. Electrochemical characterization of MFC by LSV and VR methods: (A) potential and (B) power density as a function of current density.

exchanged per mole of oxygen, ν_{An} is the volume of liquid in the anode compartment, and ΔCOD is the change in *COD* over time *t*. The obtained ε_{Cb} values for PU/Graph/PPy-$FeCl_3$, PU/Graph/PPy-APS and PU foam were 9.4, 6.9 and 4.4%, respectively, which demonstrated that microorganisms are able to use conducting anodes as an electron acceptor. Guo *et al.* [32] used anaerobic fluidized bed MFC to generate electricity using wastewater as fuel and activated carbon as electrode, they reported about 5% of coulombic efficiency, which was due to electron-transfer bacteria were incapable of converting all the available organics into electricity, therefore, the excessive substrate created favors the methanogens growth. In our case, the highest value of 9.4% of coulombic efficiency is relatively good, taking into account that municipal wastewater was used as fuel and that air was not fed to cathode chamber. When substrates as glucose or acetate are used as fuel, higher efficiencies can be achieved, as can be seen in the revision of Fornero *et al*. [33].

On the other hand, estimates of the maximum power generated in an MFC and the internal resistance can depend upon the technique used to obtain the polarization curve [34]. In the variable resistance (VR) method the circuit resistance is varied at fixed time intervals, ranging from 10 sec to 24 h. An alternative approach is sweeping the potential at different scan rates using a technique called linear sweep voltammetry (LSV) [22]. In this work, we compared the techniques of VR and LSV for determining internal resistance and polarization behavior for the characterization of a MFC using the PU/Graph/PPy-$FeCl_3$ anode, which gave the best output power density as a function of time (Fig. 6). Fig. 7 shows the electrochemical characterization of MFC by LSV and VR methods: (a) Polarization curves and (b) Power density as a function of current density. It can be observed that MFC maximum power density from PU/Graph/PPy-$FeCl_3$ anode by LSV and VR methods were ~225 mW/m^3 at a current density of 700 mA/m^3 and ~250 mW/m^3 at a current density of 1350 mA/m^3, respectively. Even when current density values at which maximum occurs were very dissimilar, difference in maximum power density value between two methods was only ~11%.

The internal resistance (R_{int}) is one of the main characteristics of a MFC, because high values tend to result in low power output of the cell. On the other hand, according to Jacobi's theorem of maximum power delivered by an electromotive force, a MFC fitted with an external resistance equal to its internal resistance will give its maximum power output [22]. Internal resistance calculated from polarization curves (Fig. 7A) by LSV and VR methods were 4.8 and 2.9 kΩ, respectively, therefore we took 3.9 kΩ as the internal resistance of MFC.

Fig. 8 shows the SEM images of the electroactive biofilm

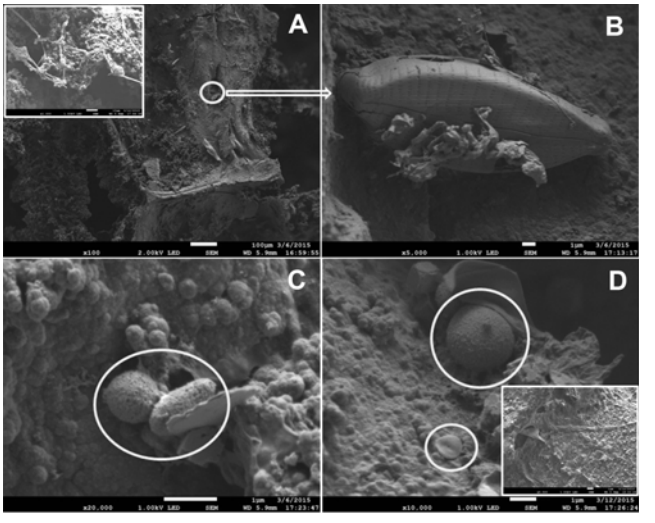

Fig. 8. Microbial colonization onto PU/Graph/PPy-$FeCl_3$ anode in anaerobic conditions.

grown on the PU/Graph/PPy-$FeCl_3$ anode after MFC operation. It can be observed that cell aggregates are formed in the anode making a thin biofilm attached to the inner surface of support. Morphologies resembling diatoms, bacillus and cocci can be observed. Although an appropriate characterization of microbial colonization of anode in the MFC was not performed, it is possible to assume that among the many bacterial species present in the bioanode there is an abundant presence of electrochemically active bacteria, considering the nature of the inoculum, the observed morphologies and the obtained power densities. Schröder [35] indicated that *Geobacter*, *Shewanella* and *Rhodoferax* are the most well-known electrochemically active microorganisms that can inhabit aquatic sediments, such as the substrate and inoculum used in our study, being *Geobacter* species the most representative because of the great variety of substrates they can utilize. For example, Yuan *et al.* [7] observed rod-shape bacterial cells attached to the surface of an anode based on polyaniline-modified natural loofah sponge in MFC with bacteria from activated anaerobic sludge. However, considerably more work is needed in order to fully characterize microorganisms in our bioanode; we are working on massive parallel sequencing analysis and the results will be published in the future.

4. Conclusion

Surface modification of PU foam coating with graphite and semiconducting PPy synthesized with APS and $FeCl_3$ as oxidizing agents, allowed their use in MFC with relatively low-cost materials (cathode catalyst-free). It was possible to generate an electrical power up to 225 mW/m^3 when $FeCl_3$ was used to polymerize pyrrole monomer, which was ascribed to higher anode conductivity and surface morphology of PPy. Internal resistance of the MFC was 3.9 kΩ as an average value calculated by two electrochemical methods (LSV and VR), with coulombic efficiency of 9.4%, which is a relatively high value taking into account that municipal wastewater was used as fuel. The low-cost MFC produced operating with PU/Graph/PPy-$FeCl_3$ as the anode gave 2.13 times more efficiency than using pure PU foam, which makes this low-cost device interesting for scaling up process not only for energy collection but also for wastewater treatment.

Acknowledgements

Author P.P.R. acknowledges the Consejo Nacional de Ciencia y Tecnología, México (Scholarship # 371995). This work was supported by the Consejo Nacional de Ciencia y Tecnología, México (Grant # SEP-80843). Author V.M.O.M. acknowledges the hospitality of Dr. L. Farías-Cepeda at the sabbatical leave in Facultad de Ciencias Químicas, Universidad Autónoma de Coahuila.

References

1. Logan, B. E. and J. M. Regan (2006) Microbial fuel cells - challenges and applications. *Environ. Sci. Technol.* 40: 5172-5180.
2. Liu, X., X. Du, X. Wang, N. Li, P. Xu, and Y. Ding (2013) Improved microbial fuel cell performance by encapsulating microbial cells with a nickel-coated sponge. *Biosens. Bioelectron.* 41: 848-851.
3. Kiely, P. D., R. Cusick, D. F. Call, P. A. Selembo, J. M. Regan, and B. E. Logan (2011) Anode microbial communities produced by changing from microbial fuel cell to microbial electrolysis cell operation using two different wastewaters. *Bioresour. Technol.* 102: 388-394.
4. Premier, G. C., J. R. Kim, I. Michie, R. M. Dinsdale, and A. J. Guwy (2011) Automatic control of load increases power and efficiency in a microbial fuel cell. *J. Power Sour.* 196: 2013-2019.
5. Xie, X., G. Yu, N. Liu, Z. Bao, C. S. Criddle, and Y. Cui (2012) Graphene–sponges as high-performance low-cost anodes for microbial fuel cells. *Energy Environ. Sci.* 5: 6862-6866.
6. Fan, Y., E. Sharbrough, and H. Liu (2008) Quantification of the internal resistance distribution of microbial fuel cells. *Environ. Sci. Technol.* 42: 8101-8107.
7. Yuan, Y., S. Zhou, Y. Liu, and J. Tang (2013) Nanostructured macroporous bioanode based on polyaniline-modified natural loofah sponge for high-performance microbial fuel cells. *Environ. Sci. Technol.* 47: 14525-14532.
8. Park, H. O., S. Oh, R. Bade, and W. S. Shin (2011) Application of Fungal Moving-Bed Biofilm Reactors (MBBRs) and chemical coagulation for dyeing wastewater treatment. *KSCE J. Civ. Eng.* 15: 453-461.
9. Deng, Q., X. Li, J. E. Zuo, B. E. Logan, and A. Ling (2009) Power generation using an activated carbon fiber felt (ACFF) cathode in an upflow microbial fuel cell. *J. Power Sour.* 195: 1130-1135.
10. Yuan, Y. and S. Kim (2008) Improved performance of a microbial fuel cell with polypyrrole/carbon black composite coated carbon paper anodes. *Bull. Kor. Chem. Soc.* 29: 1344-1348.
11. Patil, V. D., D. B. Patil, M. B. Deshmukh, and S. H. Pawar (2013) Role of modified electrode on the performance of microbial fuel cell. *Int. J. Adv. Sci. Eng. Technol.* 2: 138-143.
12. Choi, H. J., Y. M. Song, I. Chung, K. S. Ryu, and N. J. Jo (2009) Conducting polymer actuator based on chemically deposited polypyrrole and polyurethane-based solid polymer electrolyte working in air. *Smart Mater. Struct.* 18: 024006.
13. Broda, C. R., J. Y. Lee, S. Sirivisoot, C. E. Schmidt, and B. S. Harrison (2011) A chemically polymerized electrically conducting composite of polypyrrole nanoparticles and polyurethane for tissue engineering. *J. Biomed. Mater. Res. A* 98: 509-516.
14. Chiu, H. T., J. S. Lin, and C. M. Huang (1992) The morphology and conductivity of polypyrrole/polyurethane alloy films. *J. Appl. Electrochem.* 22: 358-363.
15. Bouanga, C. V., K. Fatyeyeva, P. Y. Baillif, C. Khaokong, J. F. Pilard, and M. Tabellout (2010) Dielectric relaxation phenomena and electric properties of conductive composite polyurethane/polyaniline films. *Macromol. Symp.* 290:175-184.
16. Rangel-Vázquez, N. A., R. Salgado-Delgado, E. García-Hernández, and A. M. Mendoza-Martínez (2009) Characterization of

copolymer based in polyurethane and polyaniline (PU/PANI). *J. Mex. Chem. Soc.* 53: 248-252.
17. Xie, X., M. Ye, L. Hu, N. Liu, J. R. McDonough, W. Chen, H. N. Alshareef, C. S. Criddle, and Y. Cui (2012) Carbon nanotube-coated macroporous sponge for microbial fuel cell electrodes. *Energy Environ. Sci.* 5: 5265-5270.
18. Antonio-Carmona, I. D., S. Y. Martínez-Amador, H. Martínez-Gutiérrez, V. M. Ovando-Medina, and O. González-Ortega (2015) Semiconducting polyurethane/polypyrrole/polyaniline for microorganism immobilization and wastewater treatment in anaerobic/aerobic sequential packed bed reactors. *J. App. Polym. Sci.* 132: 42242-42252.
19. Eaton, A. D., L. S. Clesceri, A. E. Greenberg, and M. A. H. Franson (1995) *Standard methods for the examination of water and wastewater.* American Public Health Association, Washington, DC, USA.
20. NMX-AA-030-SCFI-2001 (2001) *Análisis de Agua – Determinación de la Demanda Química de Oxígeno en Aguas Naturales, Residuales y Residuales Tratadas – Método de Prueba (Cancela a la NMN-AA-030-1981).* Secretaría de Economía, México.
21. Logan, B. E., B. Hamelers, R. Rozendal, U. Schröder U, J. Keller, S. Freguia, P. Aelterman, W. Verstraete, and K. Rabaey (2006) Microbial fuel cells: Methodology and technology. *Environ. Sci. Technol.* 40: 5181-5192.
22. Sathish-Kumar, K., O. Solorza-Feria, R. Hernández-Vera, G. Vazquez-Huerta, and H. M. Poggi-Varaldo (2012) Comparison of various techniques to characterize a single chamber microbial fuel cell loaded with sulfate reducing biocatalysts. *J. New Mat. Electrochem. Syst.* 15: 195-201.
23. Borole, A. P., D. Aaron, C. Y. Hamilton, and C. Tsouris (2010) Understanding long-term changes in microbial fuel cell performance using electrochemical impedance spectroscopy. *Environ. Sci. Technol.* 44: 2740-2745.
24. Kim, S. I. and S. H. Roh (2010) Multiwalled carbon nanotube/polyacrylonitrile composite as anode material for microbial fuel cells application. *J. Nanosci. Nanotechno.* 10: 3271-3274.
25. Zou, Y., C. Xiang, L. Yang, L. X. Sun, F. Xu, and Z. Cao (2008) A mediatorless microbial fuel cell using polypyrrole coated carbon nanotubes composite as anode material. *Int. J. Hydrogen Energ.* 33: 4856-4862.
26. Cheng, S. and B. E. Logan (2007) Ammonia treatment of carbon cloth anodes to enhance power generation of microbial fuel cells. *Electrochem. Commun.* 9: 492-496.
27. Yuan, Y. and S. Kim (2008) Improved performance of a microbial fuel cell with polypyrrole/carbon black composite coated carbon paper anodes. *Bull. Kor. Chem. Soc.* 29: 1344-1348.
28. Pérez-Martínez, C. J., T. del Castillo-Castro, M. M. Castillo-Ortega,D. E. Rodríguez-Félix, P. J. Herrera-Franco, and V. M. Ovando-Medina (2013) Preparation of polyaniline submicro/nanostructures using L-glutamic acid: Loading and releasing studies of amoxicillin. *Synth. Met.*184: 41-47.
29. Gregorí, B. S., M. Guerra, G. Mieres, L. Alba, A. Brown, N. A. Rangel-Vázquez, M. Sosa, and Y. de la Hoz (2008) Caracterización estructural de poliuretanos mediante espectroscopia FTIR y RMN (^{1}H y C^{13}). *Rev. Iberoam. Polim.* 9: 377-388.
30. Choi, J., H. Kim, S. Haam, and S. Y. Lee (2010) Effects of reaction sequence on the colloidal polypyrrole nanostructures and conductivity. *J. Disper. Sci. Technol.* 31: 743-749.
31. Buitron, G. and C. Cervantes-Astorga (2013) Performance evaluation of a low-cost microbial fuel cell using municipal wastewater. *Water Air Soil Poll.* 224: 2-8.
32. Guo, Q., S. Zhao, X. Wang, X. Yue, and L. Hou (2010) Electricity generation characteristics of an anaerobic fluidized bed microbial fuel cell. *The 13th International Conference on Fluidization - New Paradigm in Fluidization Engineering, Art*. 43: 1-8.
33. Fornero, J. J., M. Rosenbaum, and L. T. Angenent (2010) Electric power generation from municipal, food, and animal wastewaters using microbial fuel cells. *Electroanal.* 22: 832-843.
34. Menicucci, J., H. Beyenal, E. Marsili, R. Angathevar, G. Demir, and Z. Lewandowski (2006) Procedure for determining maximum sustainable power generated by microbial fuel cells. *Environ. Sci. Technol.* 40: 1062-1068.
35. Schröder, U. (2007) Anodic electron transfer mechanisms in microbial fuel cells and their energy efficiency. *Phys. Chem. Chem. Phys.* 9: 2619-2629.